APPENDIX B
TEST CONDUCT

APPENDIX B
TEST CONDUCT

Test RIA 1-4 consisted of a nonnuclear loop heatup phase, nuclear power calibration and fuel conditioning phase, reactor shutdown for fuel rod and flux wire replacement, loop heatup before the power burst, and the transient power burst. Instrument status checks were made before each test phase and during the loop heatups to initialize instrument readings and ensure that critical instrumentation was operable. The operational phases of the test are discussed in the following sections.

Nonnuclear Heatup Phase

The nonnuclear heatup established the following loop coolant conditions specified for the power calibration and fuel conditioning phase: 538 K for inlet temperature, 6.45 MPa for coolant pressure, and 5.45 L/s for shroud flow rate. During heatup, the chemistry of the loop coolant was adjusted within the following limits:

pH range	5.7 to 10.2
Specific conductivity	1.4 to 48 μS/cm
Dissolved oxygen	<0.1 ppm
Chlorides	<0.15 ppm
Total suspended solids	<1.0 ppm.

Instrument status checks were performed at ambient conditions before each heatup. During heatup, several more instrument status checks were performed at several loop temperatures to adjust the zero power-zero flow instrument offsets and confirm operability of the instrumentation.

Power Calibration and Fuel Conditioning Phase

The Test RIA 1-4 power calibration and test rod fuel preconditioning were conducted concurrently. The objective of the power calibration was to intercalibrate the thermal-hydraulically determined fuel rod power with reactor neutron detecting chambers and neutron and gamma flux detectors mounted on the test train. The objectives of the fuel conditioning were to build up the short-lived fission product inventory in the fuel rod and cause further fuel relocation. The reactor core power history during the combined power calibration and preconditioning phase is summarized in Table B-1. Calculated total bundle power is presented in Figure B-1.

The fuel rod bundle power calibration was accomplished by measuring coolant pressure, inlet temperature, temperature rise from the inlet to outlet, and volumetric flow rate through the shroud. Measurements of the coolant flow through the shroud surrounding the fuel rod bundle and the flow bypassing the shroud were taken for comparison with similar measurements taken after the power burst was completed. The valves on the in-pile tube (IPT) bypass line were closed for these measurements. The valves on the IPT bypass line were opened for the power burst to decrease loop and shroud flow fluctuations.

Flux Wire and Fuel Rod Replacement

After completing the power calibration and preconditioning phase, the test loop was cooled to ambient conditions and depressurized. The test train was removed from the IPT, and the eight flux wires mounted on the outer surface of the flow shroud were replaced with 100% cobalt flux wires. Rod 804-2 was replaced with Rod 804-10 to permit posttest radiochemical analysis of a fuel rod exposed only to the power burst. A radiochemical analysis of Rod 804-2 was made to calibrate the flux wires located on the flow shroud and in the core during the power calibration and preconditioning phase.

TABLE B-1. REACTOR AND BUNDLE POWER HISTORIES FOR THE POWER CALIBRATION AND FUEL CONDITIONING PHASE OF TEST RIA 1-4

Time Duration (min)	Reactor Power (MW)	Total Bundle Power (kW)
--	0	--
22	0 to 100 kW	--
13	100 kW to 7.0	--
10	7.0	73
10	7.0 to 100 kW	--
25	100 kW to 13.5	--
10	13.5	135
8	13.5 to 100 kW	--
22	100 kW to 20.4	--
16	20.4	196
15	20.4 to 100 kW	--
37	100 kW to 25.9	--
13	25.9	244
13	25.9 to 100 kW	--
19	100 kW to 3.6	--
8	3.6	38
5	3.6 to 100 kW	--
12	100 kW to 10.2	--
10	10.2	106
6	10.2 to 100 kW	--
42	100 kW to 16.8	--
10	16.8	167
19	16.8 to 100 kW	--
28	100 kW to 23.4	--
11	23.4	222
11	23.4 to 100 kW	--
13	100 kW to 6.8	--
13	6.8	72
6	6.8 to 100 kW	--
25	100 kW to 13.4	--
11	13.4	135
9	13.4 to 100 kW	--
19	100 kW to 20.1	--
10	20.1	195
11	20.1 to 100 kW	--
37	100 kW to 25.9	--
10	25.9	242
2	25.9 to 0	--

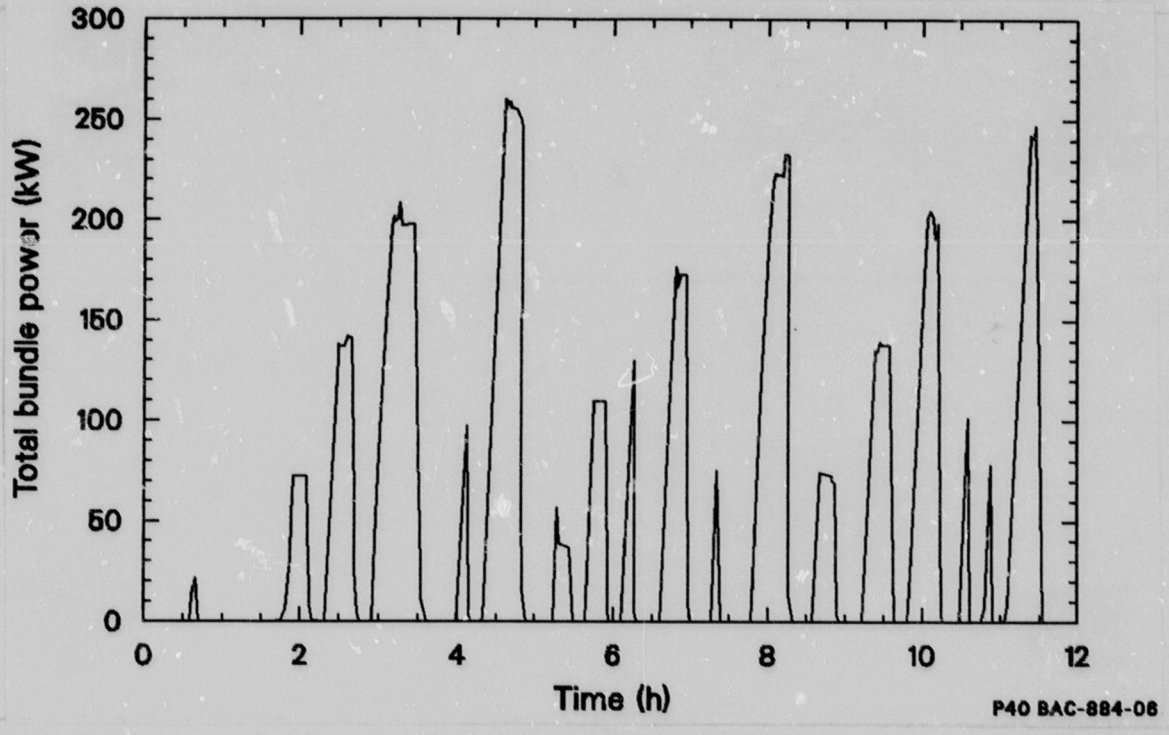

Figure B-1. Total bundle power during the power calibration and preconditioning phases of RIA 1-4.

Pre-Power-Burst Heatup Phase

During the pre-power-burst heatup phase, test coolant conditions were established at 538 K, 6.45 MPa, and 0.766 L/s. A final evaluation of the instrument readings was performed, and required adjustments made.

Power Burst Testing

After a heatup to establish the loop coolant at boiling water reactor hot-startup conditions, a single power burst with a reactor period of about 2.8 ms and a peak power of about 37,000 MW was conducted. A reactivity balance method was used to initiate the power burst. This method provides assurance that the control and transient rods have not been grossly mispositioned and no potentially dangerous reactivity addition can be made. The reactivity balance method is depicted in Figure B-2 and included the following sequence of events:

1. The control rods were withdrawn from their scram positions [Figure B-2(a)] until criticality was achieved at about 100 W and the low power critical position of the control rods was determined [Figure B-2(b)].

2. From that position, the control rods were further withdrawn until a reactor transient period of about 10 s was achieved. Then the reactor power was increased until the plant protection system was determined to be operating correctly. The control rods were then inserted until the reactor was subcritical.

3. The transient rods were inserted into the core to a position calculated for the reactivity insertion required for the power burst [Figure B-2(c)].

4. The control rods were then withdrawn again to reestablish criticality at a low power level [Figure B-2(d)]. The reactivity inserted by the withdrawal of the control rods and the worth of

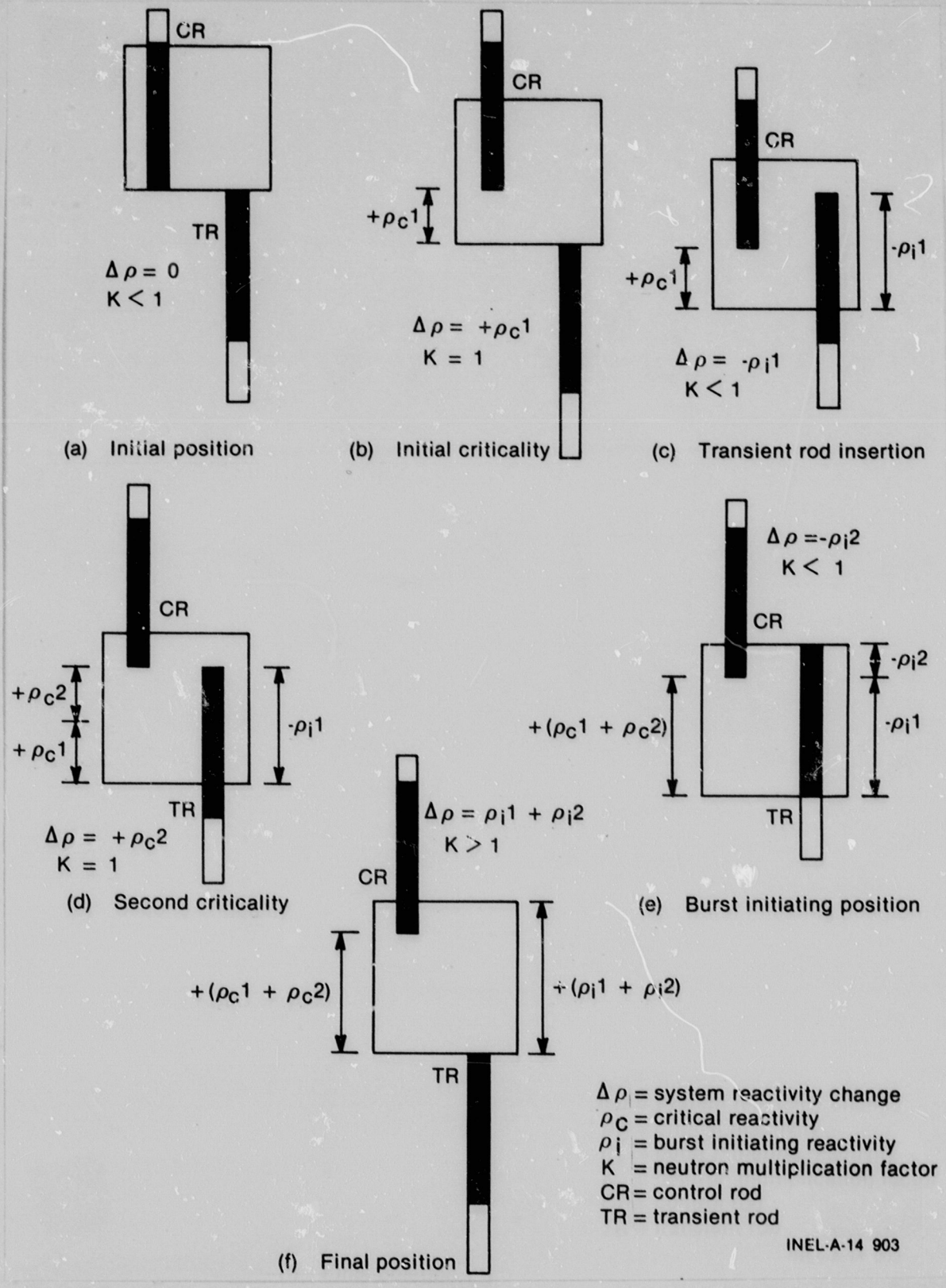

Figure B-2. Power burst testing sequence for the reactivity balance method.

the transient rods were compared for assurance that the increment of control rod withdrawal determined for the power burst was not grossly in error.

5. The control rods were adjusted to the withdrawal position for the desired reactivity insertion.

6. The transient rods were then fully inserted into the core [Figure B-2(e)].

7. To initiate the power burst, all four transient rods were ejected at a velocity of about 950 cm/s [Figure B-2(f)]. The power burst was self-terminating by the Doppler reactivity feedback, which is capable of terminating the burst without primary dependence on mechanical systems. All eight control rods were then completely inserted into the driver core to provide mechanical shutdown of the reactor.

The total bundle power during the transient is presented in Figure B-3.

Transient Energy Deposition Measurements

During a Power Burst Facility (PBF) RIA test, the reactor is operated in a natural burst mode in which a rapid increase in the core reactivity results in a large, rapid increase in the reactor power up to 100,000 MW. The prompt neutron energy deposition during the actual power burst is followed by an extended period (several minutes) of delayed neutron deposition. The delayed neutron deposition is caused by the release of delayed neutrons into the subcritical PBF core after the control rods are scrammed to terminate the power burst. The delayed component of the deposited energy was about 19% of the total energy.

Previous power burst energy measurements for closed-capsule RIA tests conducted at Capsule Driver Core (CDC) and Transient Reactor Test Facility (TREAT) were based on calibrating the activation of a neutron flux monitor with radiochemical analysis of fuel rod samples irradiated during very low power, steady-state operation or a low energy power burst. The activation

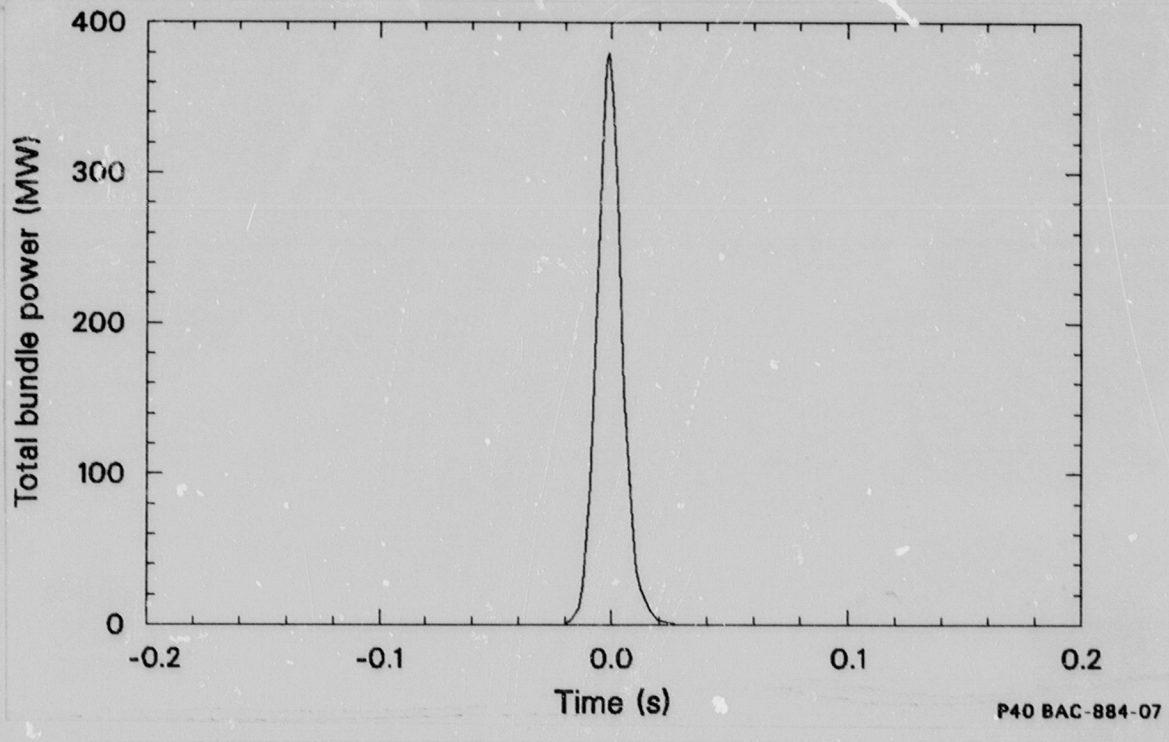

Figure B-3. Total bundle power during the RIA 1-4 transient.

of another flux monitor irradiated during the high energy power burst was then used to determine the fuel rod energy during the high energy power bursts. Radiochemical burnup analysis of fuel samples irradiated during the high energy power bursts usually was not possible because of failure over the entire length of the relatively short fuel rods. The CDC and TREAT energy data were reported in terms of total energy deposited during and after the power burst.[a] However, the test fuel rod and flux monitor remained in the reactor for several hours after each power burst. Therefore, the flux monitor measured total fissions of the test fuel rod and the delayed neutron flux. The delayed neutron flux does not significantly affect rod behavior.

For the PBF RIA tests, the unique capabilities of the facility (i.e., high steady-state power, test loop with flow capabilities, and relatively long test rods) allowed the use of different techniques to measure power burst fuel energy than were possible with the previous closed-capsule RIA tests conducted at CDC, TREAT, and the Japanese Nuclear Safety Research Reactor (NSRR). Intercalibration of the calorimetrically measured fuel rod power with core chambers and self-powered neutron detectors (SPNDs) was conducted at reactor powers up to about 26 MW. The output of the core power chambers and the SPNDs and self-powered gamma detectors (SPGDs) was then used to determine the test fuel rod energy during the power burst. Because the test fuel rods were relatively long, radiochemical burnup analysis of fuel samples above and below the failed central region of the test rods was possible. Flux wire data, calibrated with steady-state fuel burnup and corrected for delayed neutrons by reactor physics calculations, were also used to measure power burst fuel energies, similar to the previous CDC and TREAT tests.

The NRC Regulatory Guide 1.77 licensing criteria for an RIA event limits the calculated axial peak, radial average fuel enthalpy to 280 cal/g

---

a. The total fuel energy is defined as the integrated, radially averaged power produced per gram of UO_2 at the fuel rod axial flux peak, from initiation of the power burst until the rod is removed from the reactor, plus the energy equivalent to the initial fuel temperature.

for power reactors. The axial peak, radial average fuel enthalpy is defined as the maximum radially averaged UO_2 enthalpy attained at the fuel rod axial flux peak during the power burst. Probably the most important parameter for fuel rod behavior during an RIA event is the peak fuel enthalpy near the fuel pellet surface, which controls heat transfer from the fuel to the cladding and the resultant cladding temperature. The peak fuel enthalpy is defined as the maximum radial enthalpy attained at the fuel rod axial flux peak during the power burst. The FRAP-T6[a] computer code was used to determine the axial peak, radial average and peak fuel enthalpies for Test RIA 1-4 from the measured total energy depositions.

Evaluation of Measurement Methods

Evaluations of the five energy measurement methods are discussed in the following paragraphs. Stated uncertainties in this section all have a 63% confidence level.

Method 1: Core Chambers

The accuracy of test fuel rod energies determined from core power chamber data depends primarily on (a) the accuracy of the calorimetrically determined fuel rod power during the power calibration phase of the test and (b) the linearity of the core chambers and associated electronics during the power burst. Contributing error sources involved with steady-state calorimetric measurements for Test RIA 1-4 result in a typical uncertainty in measured fuel rod power of ±7%. The calorimetric measurement of steady-state fuel rod power can lead to larger error if larger systematic or random errors are present.

Because the reactor power varies from about 26 MW during the steady-state power calibration to peak powers of 37,000 MW during a power

---

a. FRAP-T6 (Fuel Rod Analysis Program-Transient) is the Idaho National Engineering Laboratory fuel performance code. FRAP-T6, Code Configuration Control Number F00404, was used for this study. See Appendix D Fuel Rod Analysis.

burst, slight errors in chamber linearity and associated electronics will affect the results. The four core power chambers are designated TR-1, TR-2, EV-1, and EV-2. Chambers TR-1 and TR-2 are of the same design and are located equidistant from the center of the core. The calculated steady-state outputs from Chambers TR-1 and TR-2 have a 0.2% neutron component, 96.7% prompt gamma component, and 3.1% delayed gamma component. Chambers EV-1 and EV-2 are of a different design than Chambers TR-1 and TR-2 and are located much closer to the center of the core. The calculated equilibrium steady-state currents from Chambers EV-1 and EV-2 consist of a 98.3% neutron component, 1.6% prompt gamma component, and 0.1% delayed gamma component. Measurements of the reactor power and energy during a power burst with Chambers TR-1 and TR-2 were corrected by 3.1% to account for the absence of delayed gammas, whereas measurements with Chambers EV-1 and EV-2 did not require correction because the delayed gamma component was negligible.

Because the two types of chambers have different neutron and gamma sensitivities, chamber linearity was evaluated during power burst core qualification tests before Test RIA 1-4 by plotting the chamber output for Chambers TR-1 and TR-2 at the time of peak power as a function of the output of Chambers EV-1 and EV-2. The linearity of the data indicates that the chambers are linear with respect to each other. This linearity of data is also good evidence that the chambers are linear in their response to the power burst radiation. The data would also be linear if both sets of chambers were becoming nonlinear at the same rate, but it is improbable that the chambers would become nonlinear at the same rate. The four core power chambers, although linear, indicated reactor powers with a spread of ±10%. This spread is primarily caused by inaccurate calibration of the chambers with the PBF Data Acquisition and Reduction System. Because of this ±10% spread in reactor power chamber outputs, an uncertainty of ±10% exists (associated with core chamber reactor power measurement) in the determination of test rod energy.

Another source of uncertainty in determining test rod power from the core chamber data is the calculation of the correction factor for fission

energy due to delayed neutron radiation generated after control rod scram. An estimated ±2% uncertainty is associated with this TWIGL[a] code calculation.

An uncertainty of ±1% is associated with the reactor physics calculated relative rod-to-rod peaking factors. When the components of uncertainty discussed previously for the determination of test rod power from core power chamber data are combined through use of the square root of the sum of the squares approach, an overall one sigma uncertainty of ±12% is obtained.

Method 2: Self-Powered Neutron and Gamma Detectors

Fuel rod energy values based on the SPND and SPGD data rely on the same calorimetric power measurements used in Method 1; therefore, a ±7% uncertainty component for calorimetric determination of rod power exists. In addition, the output of a cobalt SPND during equilibrium steady-state operation is composed of prompt and delayed neutron components, and prompt and delayed gamma components. The polarity of the gamma-induced output current for a cobalt SPND is the opposite of the neutron-induced output current. The output of an SPND for a given neutron flux is, therefore, higher during a power burst than during steady-state operation, because of the absence of a delayed gamma flux during the power burst. The SPND outputs during each power burst were adjusted by a calculated correction factor of 0.95 to account for the absence of delayed gammas during the power burst. The uncertainty in the calculation of this correction factor is ±2%.

As discussed in the evaluation of the core chamber data, another source of uncertainty exists: the calculation of a correction factor for fission energy due to delayed neutron radiation generated after control rod scram. The estimated uncertainty of this TWIGL calculation is ±2%. In addition, the calculated relative rod-to-rod power distribution uncertainty is ±1%. Because the logarithmic amplifiers connected to the SPNDs and

---

a. TWIGL, Idaho National Engineering Laboratory Code Configuration Control Number HOO99718.

SPGDs span eight decades of SPND output, small drifts in the data system electronics lead to relatively large errors in the indicated SPND or SPGD output current. Because of the electronics problems, the fuel energy values based on measurements from the SPND at 180 degrees and the SPGD at 90 degrees were disregarded in evaluating the best estimate of the fuel energy. The uncertainty due to the logarithmic behavior of the SPND amplifiers and the drift in the data acquisition system electronics is estimated to be ±12%.

The overall one sigma uncertainty for the fuel energy determined from the SPND and SPGD data, based on the square root of the sum of the squares approach to combining the uncertainty components, is ±14%.

Method 3: Shroud Flux Wires and Steady-State Burnup Analysis

Possible uncertainties related to the shroud flux wire method include the following:

- The neutron spectrum may be different during a power burst than during steady-state operation. According to reactor physics TWIGL computer code calculations, this error is negligible.

- Because the ratio of thermal neutron to resonance neutron activation of cobalt is different than the ratio of thermal neutron to reasonance neutron fission of U-235, the ratio of cobalt-measured neutron fluence values during steady-state operation and during a power burst may be different. This error has not been measured, but it is estimated to be ±4%.

- The flux wire results were normalized to the radiochemical analysis of Fuel Rod 804-7. According to Exxon Nuclear Idaho Company, Inc. radiochemical analysts, where radiochemical analyses were done, there is an estimated uncertainty of ±7% in the results.

- The uncertainty in measuring the activation of the flux wires is about ±4%. This includes uncertainties in physical constants, detector calibration, counting statistics, the cobalt content of the wires, and the contribution of impurities in the wire.

- Uncertainty in the calculated rod-to-rod relative power peaking is about ±1%.

- A potential exists for positioning errors in relating the axial location of the flux wire to the location of the fuel stack in the rods. The uncertainty of flux wire position represents an estimated ±3% uncertainty in the fuel energy measurement.

- The correction factor for fission energy generated after control rod scram contributes about ±2% to the uncertainty of fuel rod energy value.

The overall one sigma uncertainty in the shroud flux wire and burnup analysis method, obtained by combining all of the uncertainties discussed previously, is ±10%.

Method 4: Shroud Flux Wires and Calorimetric Power Calibration

The same uncertainties associated with the shroud flux wire measurements described in Method 3 exist for Method 4. The flux wire results were normalized to the integrated fuel rod bundle power determined calorimetrically, which has an estimated uncertainty of ±7%. The overall one sigma uncertainty in the shroud flux wire and calorimetric power calibration method is ±10%.

Method 5: Power Burst Burnup Analyses

Possible uncertainties in determining test rod energy during a power burst from the power burst radiochemical burnup analyses data include the following:

- Contamination of fuel samples subjected to only a power burst may occur during sectioning and handling in the hot cell when higher burnup samples are also present. The activation of fuel in the rods irradiated only during a power burst is much less than the activation of the fuel during steady-state operation. This problem was observed from burnup analyses of earlier RIA tests for several fuel samples. Improved sample preparation techniques have been implemented to eliminate this problem. The uncertainty in radiochemically determined fuel energy due to contamination is believed to be negligible for the Test RIA 1-4 analyses.

- There are potential errors in (a) cutting a sample from a specified section of a fuel rod, (b) determining the relative location of a fuel rod and the shroud flux wire, and (c) scanning the flux wire. These errors represent an estimated ±5% error in the evaluated fuel energy.

- Radiochemical analysts estimate the uncertainty in the radiochemical burnup analyses to be ±7%.

The overall estimated one sigma uncertainty in the burnup analyses, obtained by combining the uncertainty components, is ±9%. Fuel burnup analyses of a fuel rod exposed to only a power burst appear to be the best method of measuring the total adiabatic fuel energy during a power burst. The other methods must rely on thermal-hydraulic calorimetric measurements of the fuel rod power or radiochemical analyses during steady-state operation and, therefore, must be interrelated with other instruments to measure the fuel rod energy during a power burst. The burnup analyses method has the disadvantage of being limited to previously unirradiated fuel rods or previously irradiated fuel rods with low residual activity for the fission product isotope used in the analyses.

The previously irradiated MAPI[a] fuel rods used in Test RIA 1-4 had a low residual activity, because they had been in storage for about 8 yr before testing in PBF. Migration of fission products will also adversely affect the accuracy of the radiochemical analyses. Data from one of the five burnup samples were rejected because the energy deposition value was unrealistically low.

Summary of Energy Measurement Methods

Best estimates of the energy depositions, obtained by averaging the results of the specific measurement methods, and the standard deviations are summarized in Table B-2. These data represent the total radial average fission energy deposited at the axial flux peak of the test rods up to the time of control rod scram.

The five energy measurement methods had estimated 63% confidence level uncertainties ranging from ±9% to ±14%. The standard deviations for the best-estimate energy deposition values were obtained by averaging the results of the five methods. Fuel burnup analyses of a fuel rod exposed only to the power burst is considered the best method for determining the power burst fuel energy deposition. The other methods must rely on calorimetric or burnup measurements of fuel rod power during steady-state operation and, therefore, must be interrelated with other instruments to determine the fuel rod energy during a power burst.

Fuel Enthalpy Results

The NRC licensing criteria for the acceptable analysis of an RIA event states that: "Reactivity excursions will not result in a radial average

---

a. The MAPI fuel rods were built by the Westinghouse Electric Corp. and were irradiated in the Saxton reactor for The Mitsubishi Atomic Power Industries, Inc., of Tokyo, Japan.

TABLE B-2. TEST RIA 1-4 POWER BURST ENERGY DEPOSITION DATA

Fuel Rod Position	Total Radial Average Fission Energy Deposited at Axial Flux Peak (cal/g UO_2)						
	Method 1	Method 2		Method 3	Method 4	Method 5	Best-Estimate Energy Deposition and Standard Deviation
	Core Chambers	SPND at 0°	SPGD at 270°	Shroud Flux Wire and Steady-State Burnup	Shroud Flux Wire and Calorimetric Measurements	Power Burst Burnup Analysis	
Corner rods	315,286,281,314	302	282	277	276	283,322,279,283	292 ± 17
Side rods	290,263,258,289	278	259	255	254	260,296,257,260	268 ± 13
Center rod	264,240,236,263	253	237	233	232	238,270,234,238	245 ± 14

fuel enthalpy greater than 280 cal/g (1170 J/g) at any axial location in any fuel rod." Thus, axial peak, radial average fuel enthalpy is an important RIA variable. In addition, peak fuel enthalpy near the fuel pellet surface is very important in terms of fuel rod cladding damage. Because, in both cases, enthalpy is the limiting parameter, allowance must be made for heat transfer from the fuel to the cladding and reactor coolant during the RIA power transient. Because direct measurement of fuel enthalpy during a power burst is impractical, the FRAP-T6 computer code was used to calculate heat transfer in determining peak fuel enthalpies for Test RIA 1-4. Since gap closure is abrupt in RIA transients, the potential gap conductance uncertainty was minimized. The best-estimate measured total energy deposition was used as input to the FRAP-T6 code. These calculations are described in Appendix D.

Approximately 81% of the total fuel rod energy deposition occurred before the control rod scram, ∿33 ms after the time of peak power. A peak fuel enthalpy of 277 cal/g UO_2 occurred for the corner rods about 18 ms after the time of peak power.

The estimated uncertainty in calculating the peak fuel enthalpies is ±5%. The total uncertainty in the calculated peak fuel enthalpy is estimated to be ±10%. This includes an uncertainty of ±9% for the determination of total energy deposition and ±5% for the FRAP-T6 calculation.